A tale of two shrimps – Speciation and demography of two sympatric shrimp species from hydrothermal vents

Author & Affiliations

Pierre Methou[1], Shannon B. Johnson[2], John Sherrin[3,4], Chong Chen[5], Verena Tunnicliffe[6]

[1]Univ Brest, Ifremer, CNRS, Unité Biologie des Environnements Extrêmes marins Profonds, Plouzané, France

[2]Monterey Bay Aquarium Research Institute (MBARI), Moss Landing, California, USA

[3]School of Earth & Ocean Sciences, University of Victoria, Victoria, British Columbia, Canada

[4]WSP Canada, Victoria, British Columbia, Canada

[5]X-STAR, Japan Agency for Marine-Earth Science and Technology (JAMSTEC), Yokosuka, Kanagawa 237-0061, Japan

[6]Department of Biology, University of Victoria, Victoria, British Columbia, Canada

Abstract (200 words)

Hydrothermal vents are ideal natural laboratories to study speciation processes due to their fragmented distribution often with geographic barriers between habitats. Two sympatric species of *Rimicaris* shrimps occur at vents on the Izu-Bonin-Mariana volcanic arcs: *Rimicaris loihi* also found near Hawai'i and *R. cambonae* also present on the Tonga Arc. These two species are genetically very close and sometimes co-occur, raising the question of how they can remain separate if interbreeding can still happen. Here, we use barcoding and shotgun sequencing to test if hybridization still occurs. We also evaluated population demography over 10 years to assess population densities and sex ratios at some vents. Our results support *R. cambonae* and *R. loihi* as two distinct species despite sympatry throughout part of their range and presence of hybrids. Different population sex ratios between species suggest that life-history traits such as different mating systems might reinforce reproductive barriers. We also observed fluctuations in shrimp densities alongside their genetic diversity, linked to variations in hydrothermal activities over the years. We suggest that geographic isolation after a rare, historical long-distance dispersal across volcanic arcs followed by such environmentally-driven genetic fluctuations may have fostered rapid divergence by allopatry, although sympatric speciation is not excluded.

Introduction

Speciation, the process by which two species emerges from an ancestral entity, is responsible for the biodiversity we see today. The formation of distinct species arise from their reproductive isolation that can result from geographical barriers (allopatric) or ecological barriers by a specialization for distinct niches (sympatric) [1,2]. Although some cases of sympatric speciation do occur, notably in cichlids fishes and spiny mice [3–5], allopatric speciation is generally considered as the predominant form of speciation, with geographic separation at least during part of the process [6,7]. Indeed, in the absence of geographical barriers, nascent species are still capable of interbreeding and exchange genes, promoting a homogenization of their genetic pools [8]. However, efficient reproductive barriers can maintain recently diverged species despite their capacity to interbreed and prevent recombination of genomes [2]. These barriers can be prezygotic and act before fertilization such as through distinct mate choice, mechanical incompatibility during copulation, or desynchronized reproductive cycles [9–11]; post-zygotic barriers, such as non-viability and sterility of hybrids or their counter-selection in the environment, can also reinforce speciation [12,13].

Within the deep ocean, hydrothermal vents constitute fragmented ecosystems with high endemism that form isolated “islands” along oceanic ridges, volcanic arcs and back arc basins [14,15]. Within a vent field, the steep thermal and chemical gradients generated by the mixing of the vent fluid with seawater creates a variable mosaic of distinct habitats constraining the spatial distribution of faunal communities [16,17]. Chemical composition of vent fluids further differs due to the underlying geological context, with large variations even among vent fields from the same region [18,19]. Moreover, many hydrothermal vents are also relatively unstable at ecological and evolutionary timescales, with tectonic rearrangements that can establish or break existing barriers to gene flow among populations, favouring allopatric speciation followed by secondary contact where hybridization is possible [20–24]. Hence, these ecosystems provide excellent opportunities to study the role of geography and local adaptation on speciation processes in natural populations.

Among the vent endemic fauna, species of *Rimicaris* shrimps are commonly found living sympatrically in several regions, where two or three species often co-occur within the same vent fields [25–27]. In most cases, *Rimicaris* shrimps also exhibit broad geographic distributions with high genetic connectivity along mid-ocean ridges [28–30] or back-arc basins [31–33], suggesting a high dispersal potential. As with most decapods, *Rimicaris* shrimps are gonochoric brooders that maintain their eggs under their abdomen but also display a variety of reproductive cycles with seasonal or aperiodic brooding patterns [34–36]. In some *Rimicaris* species, brooding cycles were unrelated to variations of photosynthetic surface production, unlike other seasonal brooders that inhabit vents [35].

Two sympatric *Rimicaris* species co-occur at vents from the Izu-Bonin-Mariana (collectively IBM) Volcanic Arc: *Rimicaris* (formerly *Opaepele*) *loihi* and the recently described *R. cambonae* [27]. *Rimicaris loihi* is a grazer foraging on bacterial mats covering the substratum and mussel shells near active vents [36,37]. The habitat of *R. loihi* and *R. cambonae* is characterized by particularly active venting including areas of high degassing, pools of liquid CO_2 at NW Eifuku, liquid sulfur ponds at Nikko Seamount and other sites with an extensive record of historical eruptive events [18,38]. In particular, active eruptions occurred at NW Rota Volcano during each of the six visits between 2004 and 2010, before it stopped prior to the last observations in 2014 [39–42]. *Rimicaris loihi*, was also reported from distant sites including the Loihi Seamount on the southeast coast off Hawai'i [43] and at West Mata Volcano north of Tonga [44]. West Mata and Loihi are also known for their high instability with seismic and eruptive activities, both of which were recorded at Loihi in 1996 and by *in situ* observations of explosive eruptions during dives at West Mata in 2008 and 2009 [44,45].

In addition to being sympatric, *R. cambonae* and *R. loihi* are also very closely related genetically, differing by just 2% in the barcoding region of the mitochondrial cytochrome *c* oxidase subunit I (*COI*) gene fragment [27] and thus falling within the grey zone of speciation [8]. Given that these two species coexist within the same faunal assemblages, questions arise about the presence of gene flow and possible hybridization between them and, thus, the effectiveness of reproductive barriers despite the potential for reproduction. However, data on the reproductive biology of these species are limited to one single population of *R. loihi* from Suiyo collected in August 2019, that showed a largely female-biased sex ratio, and presence of many juveniles and ovigerous females [36].

This study aims to answer the following questions: 1) Are nuclear genes of *R. loihi* and *R. cambonae* concordant with mitochondria and represent separate species-level lineages? 2) Is there gene flow and hybridisation between *R. cambonae* and *R. loihi* or is there a complete reproductive isolation? 3) To what extent does the eruptive and unstable geological context affect the population dynamics of these shrimps over the years at a given site? 4) Could differences in the reproductive characteristics of these two species explain the maintenance of two closely related species in the face of possible hybridisation? And 5) What is the most likely scenario for their speciation?

Materials and Methods

Animal sampling and processing

Alvinocaridid shrimps were collected during eight oceanographic expeditions that took place between 2004 and 2023 using suction samplers or baited traps on either Remotely Operated Vehicles (ROVs) or Human Operated Vehicles (HOVs). In total, five hydrothermal vent fields from the IBM Volcanic Arc were visited once (Seamount X in 2006, Suiyo in 2019), twice (Nikko in 2006 and 2010,

NW Eifuku in 2004 and 2023) or six times (NW Rota between 2004 and 2014) (Figure 1A). Additional shrimps were collected in 2004 at Loihi Seamount near Hawai'i, the type locality of *Rimicaris loihi* and in 2009 at the West Mata volcano (Figure 1A; see Table S1 for detailed sampling information).

Specimens were preserved either in 75% ethanol or frozen whole at -80°C on-board the ship. Additional specimens from NW Eifuku in 2023 were fixed with 4% paraformaldehyde (PFA) for 3h on board and stored in in 50% phosphate-buffered saline (PBS)-ethanol solution for electron microscopy (see Supplementary Methods). We determined sex based on examination of 1st and 2nd pleopod shape and measure size of each shrimp as carapace length (CL) and/or total length (TL) following [27]. We also distinguished *R. cambonae* and *R. loihi* morphologically based on [27] in conjunction with COI barcoding for specimens collected in 2023 at NW Eifuku. For the few ovigerous females encountered, we estimated realized fecundity from egg counts and sizes.

Shrimp Abundance

On NW Rota, where vents occurred only in the upper 80 m of the summit, fine-scale mapping with an SM2000 system, good ROV navigation, and physical markers (e.g., Schnur et al. 2017) supported comparative estimates of venting extent and shrimp distribution between years. Rugged terrain and radical changes in the volcano topography hampered regular transecting and overlays. Instead, we estimated shrimp abundance by assessing the total extent of the ROV tracks in which shrimps were visible in densities greater than ~20 individuals/m^2.

DNA extraction, COI barcode amplification, and Sanger sequencing

We performed DNA extractions on 597 alvinocaridid shrimps using the 4th/5th pleopods or pieces of abdominal tissues following manufacturer's instructions of the DNeasy Blood & Tissue kit (Qiagen, Hilden, Germany). We amplified the 5' region of the *COI* gene with the Cari-COI-1F and Cari-COI-1R alvinocaridid primers [46] for shrimps collected from Nikko 2010, Suiyo 2019, and NW Eifuku 2023 (679 to 734 bp fragment) or with the COI-1f (5'-AGTAGGAACAGCCCTTAGTCTCCTA-3') and COI-1r (5'-TCCCGCTGGGTCAAAGAATGAGG-3') primers for the remaining shrimps (529 to 623 bp fragment).

We used Promega GoTaq polymerase in 25µl reactions for PCR amplifications with Cari-COI-1F and Cari-COI-1R and iProof High Fidelity DNA Polymerase (Bio-Rad) in 40µl reactions for PCR amplifications with COI-1f and COI-1r using 1 µl of the DNA template for both. We conducted PCR with the following cycle conditions: initial denaturation at 95°C for 5 min, 35 cycles of 95°C (1 min), 50°C (1 min), 72°C (2 min), followed by a final extension stage of 72°C for 7 min with Cari-COI primers or initial denaturation at 95°C for 5 min, 35 cycles of 95°C (1 min), 50°C (1 min), 72°C (2 min), followed by a final extension stage of 72°C for 7 min with the COI-1f/ COI-1r primers.

Bi-directional Sanger sequencing was conducted by Eurofins (Köln, Germany) for PCR products amplified with Cari-COI-1F/ Cari-COI-1R primers and by the High Throughput Genomics Unit (Seattle, WA, USA) for PCR products amplified with COI-1f/COI-1r primers. We edited and aligned sequence chromatograms with Geneious Prime® 2023.1.2 (https://www.geneious.com).

Haplotype networks

To assign individual mitochondrial barcodes to putative species, we used the Assemble-Species-by-Automatic-Partitioning method (ASAP) on a 529-bp alignment, a method based on the detection of "barcode gaps" [47]. We estimated median joining haplotype networks with PopART v1.7 [48,49] with default settings. We used DnaSP v6 [50] to determine the number of variable sites (*S*), the number of haplotypes (*h*), haplotype diversities (H_d), nucleotide diversities (π), average number of nucleotide differences (*k*, [51], raw genetic distance (D_a), and pairwise F_{ST} values with 1000 permutations within and among putative species and populations.

Whole Genome Shotgun and Oxford Nanopore Sequencing

Following *COI* barcoding, we next used whole genome shotgun (WGS) sequencing on a subset of animals along our sampling range to examine whether nuclear data were concordant with mitochondrial data and to explore connectivity amongst populations and lineages. We quantified genomic DNA with the DNA High-Sensitivity assay with the Qubit 2.0 Fluorometer (ThermoFisher Scientific, Waltham MA, USA) and prepared 32 individuals for WGS sequencing with the Illumina DNA Prep kit (Illumina, Inc. San Diego, CA). Sequences were generated on the Element Bio AVITI instrument at UC Davis with a paired-end 2x150 protocol. Four older specimens from NW Rota were unsuccessful and were excluded from analyses. We also sequenced one individual (Ebi13 from cruise KM23-E05) for long reads on a M1kC device from Oxford Nanopore with the PCR Sequencing kit (SQK-PSK004) on a v9 flow-cell. Details on quality filtering of Whole Genome Shotgun and Oxford Nanopore sequencings are given in Supplementary Methods.

Molecular clock calibration for mitochondrial genomes

We used the programs Beauti v10.5.0 and BEASTX v10.5.0 [52–54] to calibrate a molecular clock and the estimated divergence times between *R. loihi* and *R. cambonae.* We included all available mitochondrial genomes from alvinocaridid shrimps. We used the substitution rate for *COI* of 2.2-2.6/MY based on [55] with a GTR+I+Γ model and a relaxed uncorrelated yule prior. We ran BEASTX for 10 million generations and sampled every 1000 generations. Trees were visualized in TreeViewer v.2.2.0 [56].

Whole Genome Shotgun Sequencing: Statistics

We used the programs ANGSD, PCAngsd [57], and ngsTools v3.0 (https://github.com/mfumagalli/ngsTools), ðaði v. 2.3.7 [58] and dadi-pipeline v.3.1.7 [59] to estimate population and species differentiation, admixture, and demographic histories of populations. With ANGSD, we estimated genotype likelihoods (GL) and the minor allele frequency (MAF) to calculate the site frequency spectrum (SFS), population differentiation; (weighted and unweighted F_{ST}), and population admixture. Lacking an ancestral sequence to polarize data, we calculated Tajima's D, Waterson's Θ, and Nucleotide diversity (π) from the SFS with a 'folded' spectrum in ANGSD. We estimated population admixture of individual genotypes with NGSadmix v.32 [60] with a MAF of 0.5 and sites where at least 5 individuals had SNP data. We also used ANGSD and ngsDist [61] to calculate genetic distances among individuals for a multiple dimensional scaling analysis (MDS). We used PCAngsd to estimate principal component analyses (PCA) with a covariance matrix estimated from genotype likelihoods in ANGSD. We also used ANGSD and realSFS from each population SFS estimates to create an input file for ðaði and then formatted the input file with the perl script: realsfs2dadi.pl (https://github.com/z0on/2bRAD_denovo /blob/master/realsfs2dadi.pl). We used the dadi-pipeline two-population diversification model set script to estimate demographic parameters where we compared *R. loihi* and *R. cambonae* from Eifuku seamount where the spectra were folded [59,62]. We had large amounts of missing data so we down-sampled our projections to reflect our sample sizes of each population. Analyses were run from 10-40 replicates for four rounds each and then we compared the lowest AIC value with the Summarize_outputs.py script from dadi-pipeline to find the best fitting model. We plotted results with the Make_plots.py script. Results were visualized in the tidyverse [63] with RStudio and R [64].

Results

Distribution, densities, and habitat preference

The two species of *Rimicaris* we studied had different distributions. We found *Rimicaris loihi* at five sites on the IBM arc spread over about 1900 km and on Loihi Volcano more than 6000 km to the east (Figure 1A); it is yet unknown at seven other IBM vent sites. It was the only species of shrimp on Suiyo, Nikko, and Loihi volcanoes, although the sample size at Loihi was very small (7 individuals). *Rimicaris loihi* was the dominant species on NW Rota where, of the 332 specimens with confirmed *COI* identification, only three were *R. cambonae* (0.9%). In contrast in 2023, *R. cambonae* was the dominant species at NW Eifuku and constituted 90.3% of shrimps collected whereas, in the small 2004 sample from the same site, only two of the 25 specimens collected were *R. cambonae*. Finally, 12 *R. cambonae* were identified from the West Mata vent field in the Southwest Pacific.

R. loihi appeared most abundant on sulphur crusts at all collection sites but were also found on surfaces of andesitic lavas at NW Rota and among mussels at both NW Eifuku and Suiyo. At NW Eifuku in 2023, *R. cambonae* co-occurred with *R. loihi* within mussel beds and on bare rocks.

Repeated exploration of NW Rota vent field between 2004 and 2010 revealed that, as eruption intensity and venting varied over the years, so did the abundance of shrimps (Table 2, Figure S1). For 2004, we estimated average shrimp densities around vents to be 386 m^{-2} (n=6; SD=165); maximum adult densities exceeded 900 m^{-2} in 2009 when shrimps were most abundant (Figure 2B). In the rugged terrain, it was not possible to map the distribution of shrimp species, but during each visit we transited along the known sites where the abundance of shrimps mirrored the venting extent, peaking in 2009 at 45%. The lowest abundances of shrimps were in 2006 during intense eruptions when shrimps were tightly clustered around a few vent openings, and in 2014, when volcanic activity had ceased and hydrothermal venting contracted to the central eruption pit (Table 2).

COI haplotype network and genetic diversity

Our ASAP analysis to assess putative species revealed two partitions that had equal support (lowest ASAP score of 2.50; Figure S2): individuals fell into either two or three genetic groups. Our morphological identifications agreed with two groups corresponding to *Rimicaris loihi* and *R. cambonae*. The third *COI* lineage identified in the three partitions result was formed by the divergence of two *R. cambonae* haplotypes from NW Rota from the rest of the *R. cambonae* haplotypes. Distribution of pairwise differences was bimodal with two distinct Gaussian distributions and showed no overlap (Figure S2). F_{ST} values also supported genetic differentiation for two groups, and possibly a third, with high values between *R. cambonae* and *R. loihi* and, to a smaller extent, between *R. cambonae* from NW Eifuku and from NW Rota (Table S2). The partitions were evident despite relatively low genetic distance (D_a = 0.023 between *R. cambonae* and *R. loihi*; D_a = 0.009 between *R. cambonae* from NW Eifuku and NW Rota).

Species delineation was also clear based on the *COI* haplotype network; it comprised 158 haplotypes from 597 barcoded individuals, of which 134 were assigned to *R. loihi* and 24 to *R. cambonae* (Figure 1D). *Rimicaris loihi* and *R. cambonae* showed distinct genetic characteristics with a much lower haplotype diversity for *R. cambonae* compared to *R. loihi* (H_d = 0.499 ± 0.052 and H_d = 0.877 ± 0.011, respectively) and almost three-fold lower nucleotide diversity for *R. cambonae* (π = 0.00190 and π = 0.00437; Table S3). Similarly, the average number of nucleotide differences was lower for *R. cambonae* (k= 1.048) than for *R. loihi* (k= 2.208) although these patterns could simply be a result of different sample sizes. The West Mata population of *R. cambonae* had higher levels of haplotype diversity (H_d), nucleotide diversity (π), and average nucleotide differences (k) compared to northern *R.*

cambonae populations (Table S3) also with two intermediate haplotypes, although closer to *R. cambonae* than *R. loihi* (Figure 1D). Haplotype variability among populations of *R. loihi* was notably higher than the sympatric *R. cambonae*, where Suiyo was the most diverse and Nikko was the least diverse (Table S3).

To explore temporal metapopulation dynamics of *R. loihi*, we estimated a separate haplotype network and summary statistics for NW Rota data only (Figure 2A). Yearly data were similar except for 2006 and 2014 when there was slightly lower nucleotide diversity (π), as well as lower average nucleotide differences (k); (Table S4).

Mitochondrial Genome clock calibration

We aligned 26 mitochondrial genomes from *R. cambonae* and *R. loihi* that we recovered from WGS data. Mitochondrial genomic alignments showed the same pattern of divergence between the two species as the *COI* fragment and differed by 1.5% for the GTR substitution model. The mitochondrial genomes of both species had the same gene composition and arrangement as all other published mitochondrial genomes of the Alvinocarididae (Figure S3). Molecular clock calibrations showed *R. cambonae* and *R. loihi* diverged relatively recently ~0.04 Mya (0.002–0.092 HPD). However, these estimates were perhaps problematic because estimates for divergence of other genera such as *Rimicaris* and *Alvinocaris* were much more recent than published accounts for a fragment of *COI.*

Whole Genome Shotgun Sequencing, species delineation, and gene flow

Our WGS sequencing for 28 *Rimicaris* individuals resulted in 109 million reads that included 20 *R. loihi* from NW Eifuku, Suiyo, and Nikko seamounts and eight *R. cambonae* from NW Eifuku (Figure 3A).

We used genomic data to assess whether nuclear loci were concordant with mitochondrial data that *R. loihi* and *R. cambonae* represented distinct species, and to infer demographic histories of the two species. Population genomic results for PCA and MDS both showed clusters for *R. loihi* and *R. cambonae* with two putative hybrids from NW Eifuku. One 'hybrid' individual had the *R. loihi* mitotype and the other had the *R. cambonae* mitotype (Figures 3 and S4). Summary statistics including Tajima's D, Watterson's θ, and nucleotide diversity were most similar for *R. loihi* from Nikko and Suiyo, but differed between the two species from NW Eifuku. We found all populations had positive values for Tajima's D. We also found that *R. loihi* from NW Eifuku had a very narrow range for Watterson's θ and nucleotide diversity compared to the other populations (Figure S5).

We estimated admixture plots from two to five populations that revealed sharp subdivision between the species, with admixed genotypes for the same two 'hybrid' individuals. Admixture plots

for three or more populations showed that *R. loihi* from NW Eifuku appeared somewhat divergent (Figure S4). However, weighted and unweighted F_{ST} estimates showed that while species were differentiated, populations of each were not (Table S5).

We used ∂a∂i to estimate the demographic histories of each species and population, however, we had a large amount of missing data and the results must be interpreted with caution. We used the AIC to determine and plot the four most probable models from analyses. Despite the distinct lineages we found that three of the four most probable models involved 'symmetric migration' and even when directional migration was tested, it also was relatively symmetric (Table S6, Figure S6). Demographic estimates from ∂a∂i analyses also showed each species had relatively similar effective population sizes for most models (Table S6, Figure S7).

Symbiont colonization, population sex ratio and reproductive traits

Scanning electron microscopy revealed distinct patterns of symbiont colonization for the "head" cavity between the two species (Figure S8). The anterior third of *R. cambonae* "head" cavities were densely colonized by filamentous bacteria with little colonization on the rest of the cavities whereas only a few sparse filamentous and rod-shaped bacteria occupied the entire "head" cavities of *R. loihi*.

The sex ratio of *R. loihi* from NW Rota was significantly female skewed for each year (χ^2 = 25.64 – 259.69, $p < 0.001$; Table 1) as previously observed in the Suiyo population [36]. A similar trend occurs for the sex ratio of *R. loihi* from NW Eifuku, but was not statistically supported (χ^2 = 1.33, $p > 0.05$) probably due to a low sample size (Table 1). Conversely, the sex ratio of *R. cambonae* from NW Eifuku did not significantly deviate from 1:1 (χ^2 = 1.09, $p > 0.05$; Table 1). Despite large sampling sizes, ovigerous females of *R. loihi* were nearly absent from populations collected at NW Rota in March (2004 and 2009) and April (2006 and 2010) with only two ovigerous females out of 408 females in these years (Figure 4A). Similarly, no ovigerous females were collected among the 72 females of *R. cambonae* from NW Eifuku in March 2023 (Figure 4A). Conversely, four ovigerous females out of 380 females were collected at NW Rota in December 2014 (Figure 4A) and larger numbers were observed peripheral to venting (but not sampled; Figure 4B). With 110 to 387 eggs per brood (11.4 to 44.4 eggs mm^{-1}), relative fecundities of *R. loihi* ovigerous females from NW Rota were in the range reported at Suiyo with 61 to 356 eggs per brood (10.2 to 49.2 eggs mm^{-1}), (Figure 4C) [36].

Discussion

How do *Rimicaris loihi* and *R. cambonae* maintain genetic segregation?

Nuclear genomic data confirmed previous results based on the mitochondrial *COI* fragment and morphology that *Rimicaris loihi* and *Rimicaris cambonae* constitute two separate species [27] that recently diverged ~0.04 Mya (0.002–0.092 HPD). Yet, we found symmetric gene flow between the two

species, as evidenced by the identification of two putative hybrids with maternal inheritance from both *R. loihi* and *R. cambonae* at NW Eifuku where they live in sympatry. Hydrothermal vents are favourable contexts for hybrid zones between closely related species, as observed for *Bathymodiolus* mussels on the East Pacific Rise and the Mid-Atlantic Ridge [20,65] and for *Lepetodrilus* limpets at the Woodlark Basin in the Southwest Pacific [66]. However, unlike these species that co-occur and hybridize at the edges of their respective geographical ranges, *R. loihi* and *R. cambonae* represent an unusual case of closely related sister-species that coexist near the centre of their distribution ranges with ongoing hybridization.

Theoretical modelling of the "tension zone" predicts that maintenance of species coexistence despite introgression often results from a balance between recurrent influx of individuals from pure parental populations from both species and selection against hybrids [67]. Under this scenario, Mariana Arc vent fields would represent a large hybrid zone stabilized by larval immigrants from pure parental populations of *R. loihi* located further north, dispersing from Suiyo and Nikko on the Izu-Bonin Arc. However, the presence of a similarly regular gene flow from a pure parental population of *R. cambonae* remains unclear. Our genetic analyses show that previous reports of *R. loihi* at West Mata volcano [44], are, in fact, referable to *R. cambonae*. Thus, this vent field on the Tonga Arc, 5600 km southeast of the nearest vent on the Mariana Arc, constitutes the only known potential locality for a pure parental population for *R. cambonae*. Within the West Pacific, few hydrothermal vent species distributions cross the equator [14] with notable exceptions such as *Alvinocaris dissimilis* shrimps or *Bathymodiolus septemdierum* mussels [33,68]. Larval dispersal among distinct volcanic arc systems or back-arc basins in the region is inferred to be infrequent and directional, following oceanic currents [14,69]. However, sustained dispersal from south to north hemisphere by larvae is inhibited by the Equatorial Counter-current and deemed highly improbable, even from the two closest locations [69]. Therefore, it is unlikely that significant gene flow exists between the two regions unless unknown sites exist to form a dispersal corridor.

Speciation between these two *Rimicaris* shrimps could be maintained by strong reproductive barriers. Differences in reproductive mode – egg laying versus brooding – likely strengthen strong reproductive isolation between the syntopic sister species of intertidal snails *Littorina saxatilis* and *L. arcana* [70]. In coastal isopods of the *Jaera* species complex, sexual isolation between co-occurring species is reinforced by preferential mate choice despite some level of hybridization [11] while receiving no influx from pure parental populations [71]. As previously reported for Suiyo [36], the samples of *R. loihi* from the Mariana Arc were largely biased toward females whereas the proportion of males and females was roughly equal for *R. cambonae*. Variation in adult sex ratios can strongly influence breeding systems and mate choice in many animal groups [72,73]. The discrepancy between

the sex ratios of *R. loihi* and *R. cambonae* may reflect different mate choice systems that limits heterospecific mating pairs. Partially desynchronized reproductive periods between *R. loihi* and *R. cambonae* could also act as an additional reproductive barrier, although evidence is limited. As with most carideans [74], alvinocaridid shrimps are gonochoric species that mate and brood their eggs under their abdomen until larval release [35,36]. However, a wide variety of reproductive cycles occurs in this family including aperiodic or periodic brooding patterns and with or without synchronicity to seasonal variations [34–36]. Taken together, current data on the brooding cycle of *R. loihi* do not seem to indicate any particular periodicity, with large numbers of ovigerous individuals in both August and December, despite a notable and repeated absence in March/April. However, there may be local variation between vent fields from different latitudes, for example, a brooding period in summer at Suiyo and in winter at NW Rota. Additional sampling at different periods is required to determine whether reproductive patterns of *R. cambonae* differ from its sister species.

Which speciation mode between *R. loihi* and *R. cambonae*?

Our observations over 10 years showed significant changes in the abundance of shrimps that reflected eruptive events and fluctuation of venting activities at NW Rota vent field. There were concomitant variations in genetic diversity that increased and contracted on a short timescale. This geological instability of some hydrothermal vent fields on the IBM volcanic arc [18,38] also characterizes vent fields on Loihi and West Mata [44,45]. The absence of both *R. loihi* and *R. cambonae* at several IBM vent sites [75] and on other volcanic arcs of the SW Pacific [14,75] suggests that these two species have specific habitat requirements and/or settlement cues related to volcanic emissions or sulphur substratum. The recent split of the two species (0.002–0.092 Mya) does not correspond to major tectonic events in the Northwest Pacific: current Mariana Arc volcanism initiated 3 – 4 Mya while volcanic activity on the Izu-Bonin Arc dates from ~25 Mya [76]. Similarly, along-arc splitting and rifting events in the Southwest Pacific, such as the opening of the Lau basin (∼5 Mya) [77,78], all significantly pre-date our mean divergence estimate between the two shrimp species (~0.04 Mya). This estimate based on mitochondrial genomes, that were less divergent than *COI,* was very recent compared to previous phylogenies [55,79]. However, these previous phylogenies calibrated the origin of Alvinocarididae using the Jurassic fossil *Harthofia* which has since been removed from Alvinocarididae as 'family uncertain'; currently no fossils are available in this family for calibration [80]. Our method also has a caveat that we apply the estimated rate for *COI* to the whole mitogenome, but despite this the separation between *R. cambonae* and *R. loihi* should not be older than a few million years. A rare circumstance of long-distance dispersal between the two distant arcs could have established an outpost population that gradually diverged from the ancestral genetic pool, driven by local fluctuations of venting activities affecting shrimp population sizes within each region as observed at NW Rota.

Therefore, the current sympatric distribution of both *R. loihi* and *R. cambonae* in the Mariana Arc would result from a secondary contact by another rare larval dispersal event from south to north. This scenario of speciation by allopatry postulates that genetic exchanges via larval dispersal between the two regions was disrupted for a sufficiently long period to generate an isolation phase. However, our demographic analyses (supplementary material, figure S6-7) suggest that our data best fitted a speciation model with symmetric migration, even if caution should be exercised due to the amount of missing data.

A speciation mechanism between *R. loihi* and *R. cambonae* with migration would imply a larval supply maintained between regions throughout their separation. High genetic connectivity over long distances has been observed in many alvinocaridid shrimps [30–33], for example, *R. exoculata* lacks genetic structure over 7100 km, likely supported by Mid-Atlantic Ridge ocean circulation promoting connectivity [28]. Morphological features of hatched larvae from several alvinocaridid species including *R. loihi* supports a long pelagic larval duration (PLD) [36,81]. We can therefore assume that *R. loihi* and *R. cambonae*, like their common ancestor, have a high dispersal potential. That potential is demonstrated by the presence of a distal outpost of *R. loihi* on Loihi Volcano near Hawai'i, likely advected from the IBM Arc by the dominant eastward current of the North Pacific Drift. However, prevailing ocean currents and a 5600 km cross-equator distance remain a major barrier to connectivity for frequent larval exchange in the western Pacific. Conversely, a similar pattern of speciation with a maintained gene flow would also appear if divergence between species had arisen without geographic isolation in sympatry.

Although debated, sympatric speciation in some species, including cichlid fishes and mice [3–5], is supported by theory suggesting that speciation in sympatry is favoured by disruptive selection for distinct ecological niches, diets and selection on mating related traits [6]. Hydrothermal vents generate steep environmental gradients occupied by different species [16,17] that could support species divergence. However, the presence of *R. loihi* and *R. cambonae* in the same habitats (mussel beds and sulphur-coated rocks) suggests divergence in discreet ecological niches is unlikely. Thus, in addition to assortative mating (see discussion above), disruptive selection between *R. loihi* and *R. cambonae* could have been driven by trophic niche differentiation, as observed in many co-occurring alvinocaridids [33,46]. Microscopic observations of their "head" cavity showed different degrees of colonization by filamentous ectosymbionts that could provide an additional feeding source of a mixed diet for *R. cambonae* while *R. loihi* would rely on bacterial mat grazing (Figure S8; Methou et al. in prep). Acquisition of a larger pool of filamentous ectosymbionts for nutrition could have driven trophic niche differentiation between vent shrimps and ultimately, participate in an ecologically driven speciation process. Further studies using larger genomic dataset across the entire range of the two

species as well as investigations on their trophic and reproductive ecology will be required to clarify mechanisms leading to their speciation.

Conclusion

We have shown that *Rimicaris loihi* and *R. cambonae* are two distinct, recently diverged species living in sympatry throughout a part of their geographic range. Analysing genetic data from shrimps collected from a single vent over a decade revealed high flexibility in genetic diversity alongside local eruption events, showing that the population dynamics of these shrimps are impacted by their unstable habitats. The detection of two hybrid individuals point to the lack of complete separation of the two species, and we suggest that the difference in sex ratios between the two species may reflect difference in mate choice as a reproductive barrier, among other possibilities. Although our demographic analyses with the data available remain inconclusive as to how speciation occurred, the geographic overlap and recent divergence of this species pair makes them an interesting case study for a future, deeper dive into speciation mechanisms that may provide insights to how species arise in insular habitats overall.

Acknowledgments

We thank Dr. Craig Moyer for providing shrimp specimens from Loihi Seamount and Dr. Timothy M. Shank for specimens from West Mata volcano. Captain and crew of R/Vs *Yokosuka*, *Kaimei,* and *Natsushima* are gratefully acknowledged for their continued support of our scientific activities during the cruises YK19-10, KM23-E05, and NT10-13 Leg 2, respectively. We extend this to the pilots and technical teams of HOVs *Shinkai 6500* and *Pisces V*, as well as ROVs *Hyper-Dolphin, KM-ROV, Jason-2,* and *ROPOS*. This is a GACHINKO Cruise Episode I (19-10) output, and we thank the GACHI-participants for their help in sorting shrimp specimens on-board. We thank the cruise chief scientists Ken Takai (JAMSTEC; YK19-10, KM23-E05) and Shinji Tsuchida (JAMSTEC; NT10-13 Leg 2) as well as Shinsuke Kawagucci (JAMSTEC) whose successful cruise proposal led to the sampling on the Mariana volcanic arc during cruise KM23-E05. Sampling during cruise KM23-E05 within the Islands Unit of the Mariana Trench Marine National Monument of the United States of America was carried out under the special use permit SUP 12542-23001 (MSR U2022-047). We are grateful for collections during several cruises in the NOAA Ring of Fire series of the Vents Program on the Mariana Volcanic Arc. Chief Scientists Bob Embley, Bill Chadwick and Dave Butterfield were critical to the output.

Funding

PM was supported by ISblue project, Interdisciplinary graduate school for the blue planet (ANR-17-EURE-0015) and co-funded by a grant from the French government under the program "Investissements d'Avenir" embedded in France 2030. PM also benefited from French State aid managed by the National Research Agency under France 2030: ANR-22-POCE-0007. Whole Genome Shotgun Sequencing was funded by the David and Lucile Packard Foundation at MBARI.

Data Availability.

All COI barcode sequences have been deposited in GenBank under accession numbers DQ328819 – DQ328837 and PQ643496 – PQ643653 (see Table S7 for details on haplotype numbers and localities with associated individual ID). Raw sequences of the WGS sequencing dataset are available in the NCBI SRA repository with the BioProject ID PRJNA1197504 (Accession numbers: SAMN45807939 – SAMN45807966). Details information on sampling localities, sampling date, sex, life stages and sizes of individuals analysed for population sex ratio and reproduction are compiled in a table sheet named “Population_dataset” in supplementary material.

Figure Captions

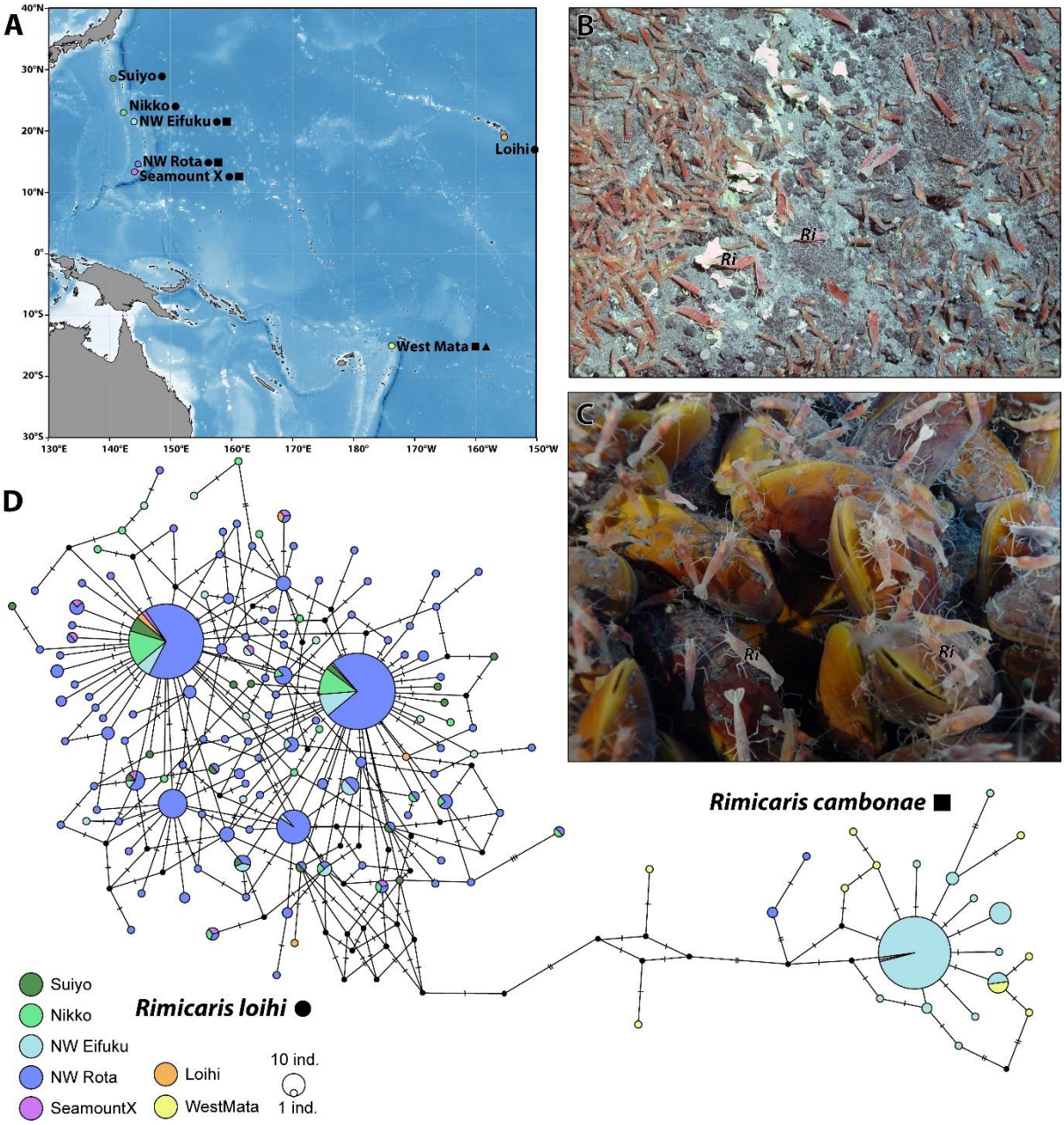

Figure 1. A. Geographic distribution of *Rimicaris cambonae* (square) and *Rimicaris loihi* (circle). Colours indicates sites and shape indicates species. **B.** and **C.** Typical habitats of *Rimicaris spp.* (*Ri*) on (**B**) sulfur crusts (NW Rota, 2009) and (**C**) mussel beds (NW Eifuku, March 2004). **D.** *COI* haplotype network (529 bp) of *Rimicaris* species from Loihi, West Mata and the Mariana Arc vent fields (n= 597) detailed per sampling site. Two clusters emerge with 24 haplotypes affiliated with *R. cambonae* and 134 haplotypes affiliated with *R. loihi*.

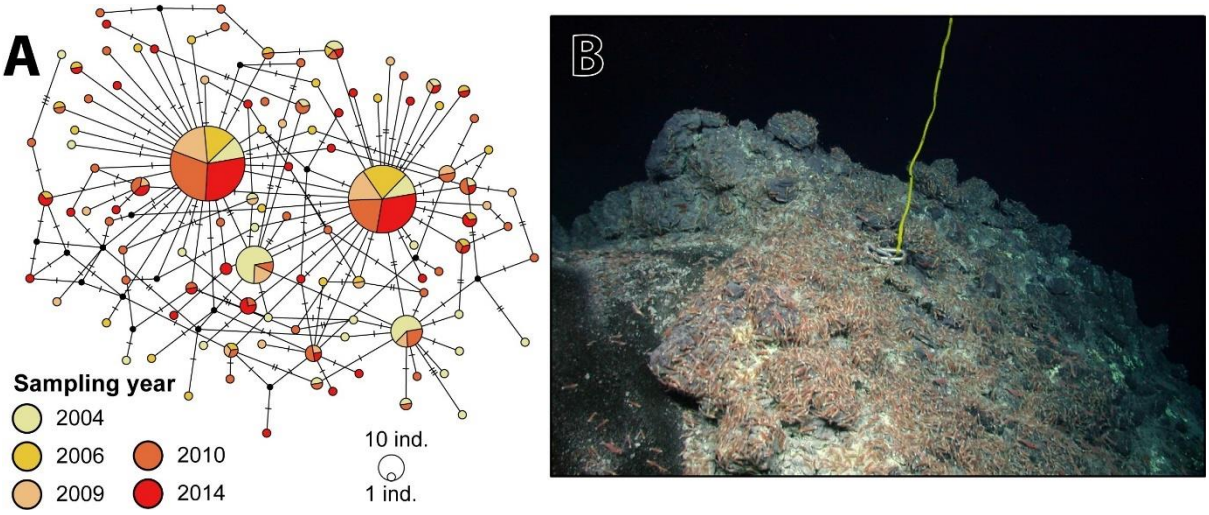

Figure 2. Temporal metapopulation dynamics of *Rimicaris loihi* at NW Rota between 2004 and 2014. **A.** *COI* haplotype network of *Rimicaris loihi* from NW Rota (n= 332) detailed per sampling year. **B.** Abundant shrimps near Marker 109 in April 2009.

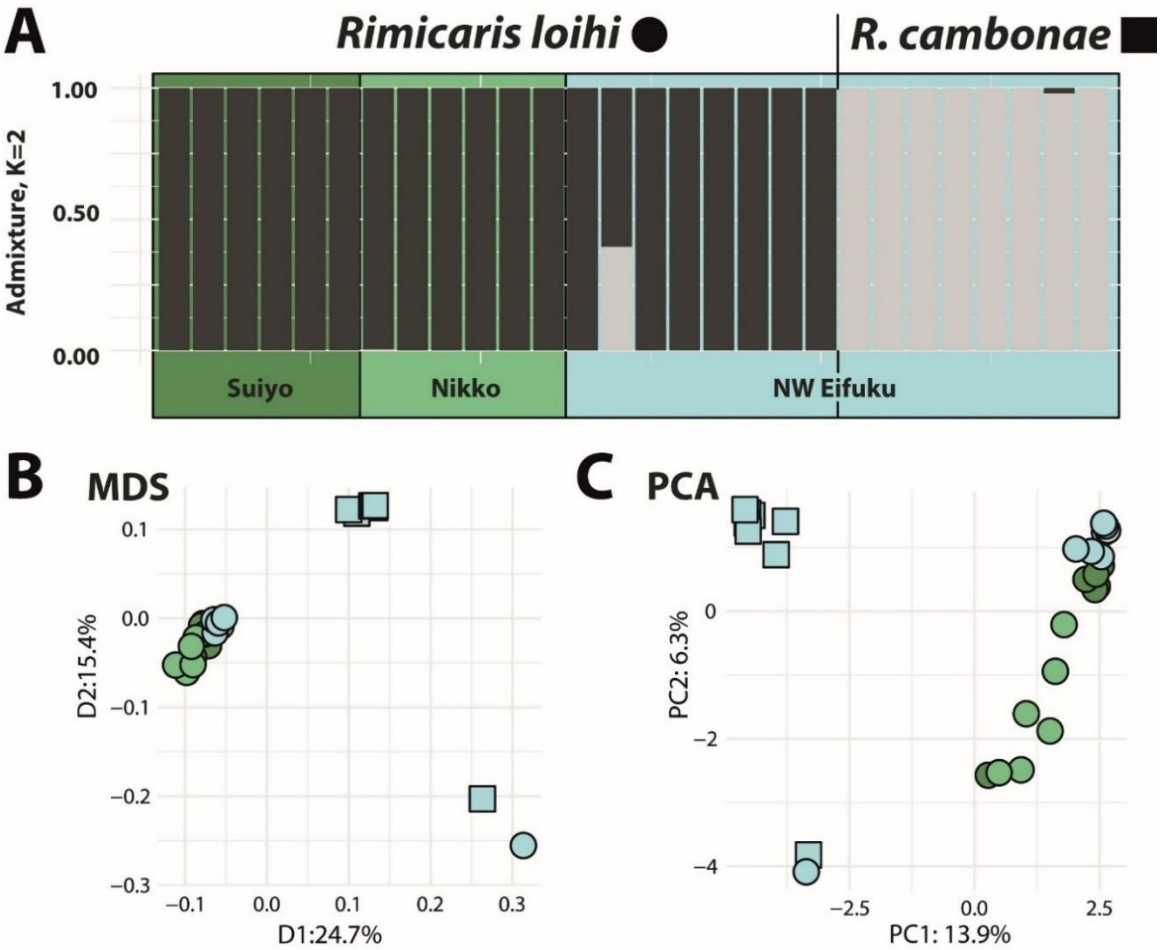

Figure 3. A. Admixture plot for two populations (K=2) including 28 individuals for 4028 loci; circles are *R. loihi* and squares are *R. cambonae,* **B.** plot of first two dimensions for multiple dimensional scaling (MDS) estimates from 4599 loci based on genetic distances, and **C.** plot of first two axes of principal component analyses (PCA) for 4178 loci. Two putative hybrids fall separately in latter two plots.

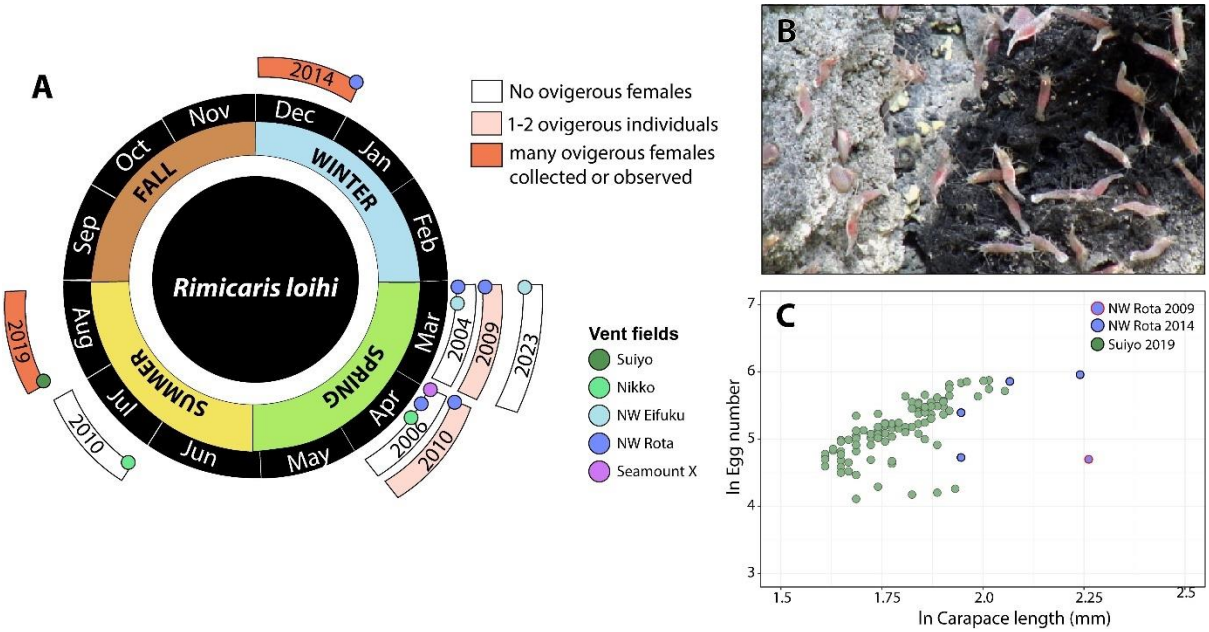

Figure 4. Reproductive characteristics of *Rimicaris loihi*. **A.** Diagrams summarizing the occurrence of *R. loihi* ovigerous females over sampling realized between 2004 and 2019. **B.** Numerous ovigerous females (reddish colour below the abdomen) observed, but not collected, at NW Rota in December 2014. **C.** Relative fecundity of *R. loihi* displayed by $\log_e$-transformed number of eggs with $\log_e$-transformed carapace length (CL). Data from Suiyo are from Methou et al. (2023). Data from NW Rota are from this study.

Vent field	Year	Species	M	F	M:F	χ^2	*p*
NW Rota	2009	*Rimicaris loihi*	119	211	0.56	25.65	***
NW Rota	2010	*Rimicaris loihi*	395	797	0.49	135.57	***
NW Rota	2014	*Rimicaris loihi*	47	380	0.12	259.69	***
Suiyo[(1)]	2019	*Rimicaris loihi*	145	235	0.62	22.94	***
NW Eifuku	2023	*Rimicaris loihi*	4	8	0.5	1.33	NS
NW Eifuku	2023	*Rimicaris cambonae*	60	72	0.83	1.09	NS

Table 1. Population characteristics with sex ratio of *Rimicaris cambonae* and *Rimicaris loihi* from NW Rota, Suiyo and NW Eifuku. [(1)] Data from Suiyo are from Methou et al. (2023). M: males, F: females; Significance levels: NS: > 0.05, *: < 0.05, **: < 0.01, ***: < 0.00.

Year	Volcanic state	Hydrothermal State	Shrimp population
2004	Volcanic vent in a deep pit with surging sulphurous plume and ejecta; mass wasting on volcano flank.[1]	13 discrete low temperature vents and seeping around rim of volcanic pit.	Extensive: dense at vents and scattered across summit; 37%
2006	Explosive eruptions from pit observed after sidewall collapse; ejecta volume to 100 m^3/hr.[2]	Discrete sites fewer; seeping through sediments near pit; eastern scarp more focussed.	Restricted: scattered near pit; concentrated at three sites; 12%.
2009	Up to 47 m of tephra accumulated since 2004[3]; ejecta evident.	Many discrete venting sites <50°C broadly distributed across summit; venting through sediments.	Very extensive: dense at vents and scattered across summit; 45%
2010	Recent eruption reshaped the summit[3]; now several volcanic orifices	Loss of several vents in landslide; exposed walls covered with sulphur;	Very extensive: dense at vents; scattered on summit and on new exposed walls; 40%.
2014	No eruptive activity[4]; likely quiescence >1 year.	No or negligible activity at all former sites; only notable temperature anomaly around pit.	Restricted mostly to one site; other locations limited or abandoned; 6%.

Table 2. History of observed volcanism and venting on NW Rota. The relative extent of the shrimp populations is assessed by estimating the % of ROV tracks in which shrimp were greater than 20 individuals/m^2. [1]Embley et al. 2006; [2]Chadwick et al. 2008; [3]Chadwick et al. 2012; [4]Schnur et al. 2014.

References

1. Coyne JA, Orr AH. 2004 *Speciation*. Sunderland, Massachusetts: Sinauer Associates.

2. Schuler H, Hood GR, Egan SP, Feder JL. 2016 Modes and Mechanisms of Speciation. *Reviews in Cell Biology and Molecular Medicine* **2**.

3. Hadid Y, Pavlíček T, Beiles A, Ianovici R, Raz S, Nevo E. 2014 Sympatric incipient speciation of spiny mice *Acomys* at "Evolution Canyon," Israel. *Proc. Natl. Acad. Sci. U.S.A.* **111**, 1043–1048. (doi:10.1073/pnas.1322301111)

4. Malinsky M *et al.* 2015 Genomic islands of speciation separate cichlid ecomorphs in an East African crater lake. *Science* **350**, 1493–1498. (doi:10.1126/science.aac9927)

5. Poelstra JW, Richards EJ, Martin CH. 2018 Speciation in sympatry with ongoing secondary gene flow and a potential olfactory trigger in a radiation of Cameroon cichlids. *Molecular Ecology* **27**, 4270–4288. (doi:10.1111/mec.14784)

6. Bolnick DI, Fitzpatrick BM. 2007 Sympatric Speciation: Models and Empirical Evidence. *Annu. Rev. Ecol. Evol. Syst.* **38**, 459–487. (doi:10.1146/annurev.ecolsys.38.091206.095804)

7. Yang M, He Z, Shi S, Wu CI. 2017 Can genomic data alone tell us whether speciation happened with gene flow? *Molecular Ecology* **26**, 2845–2849. (doi:10.1111/mec.14117)

8. Roux C, Fraïsse C, Romiguier J, Anciaux Y, Galtier N, Bierne N. 2016 Shedding Light on the Grey Zone of Speciation along a Continuum of Genomic Divergence. *PLoS Biology* **14**, 1–22. (doi:10.1371/journal.pbio.2000234)

9. Sota T, Kubota K. 1998 Genital lock-and-key as selective agent against hybridization. *Evolution* **52**, 1507–1513. (doi:10.1111/j.1558-5646.1998.tb02033.x)

10. Santos H, Rousselet J, Magnoux E, Paiva M-R, Branco M, Kerdelhué C. 2007 Genetic isolation through time: allochronic differentiation of a phenologically atypical population of the pine processionary moth. *Proc. R. Soc. B.* **274**, 935–941. (doi:10.1098/rspb.2006.3767)

11. Ribardière A, Pabion E, Coudret J, Daguin-Thiébaut C, Houbin C, Loisel S, Henry S, Broquet T. 2021 Sexual isolation with and without ecological isolation in marine isopods *Jaera albifrons* and *J. praehirsuta*. *J of Evolutionary Biology* **34**, 33–48. (doi:10.1111/jeb.13559)

12. Rundle HD. 2002 A Test of ecologically dependent postmating isolation between sympatric sticklebacks. *Evolution* **56**, 322–329. (doi:10.1111/j.0014-3820.2002.tb01342.x)

13. Arnegard ME *et al.* 2014 Genetics of ecological divergence during speciation. *Nature* **511**, 307–311. (doi:10.1038/nature13301)

14. Tunnicliffe V, Chen C, Giguère T, Rowden AA, Watanabe HK, Brunner O. 2023 Hydrothermal vent fauna of the western Pacific Ocean: Distribution patterns and biogeographic networks. *Diversity and Distributions* , ddi.13794. (doi:10.1111/ddi.13794)

15. Beaulieu SE, Szafrański KM. 2020 InterRidge Global Database of Active Submarine Hydrothermal Vent Fields Version 3.4. (doi:10.1594/PANGAEA.917894)

16. Podowski EL, Ma S, Luther GW, Wardrop D, Fisher CR. 2010 Biotic and abiotic factors affecting

distributions of megafauna in diffuse flow on andesite and basalt along the Eastern Lau Spreading Center, Tonga. *Marine Ecology Progress Series* **418**, 25–45. (doi:10.3354/meps08797)

17. Cuvelier D, Pierre-Marie Sarradin, Sarrazin J, Colaço A, Copley JT, Desbruyeres D, Glover AG, Santos RS, Tyler PA. 2011 Hydrothermal faunal assemblages and habitat characterisation at the Eiffel Tower edifice (Lucky Strike , Mid-atlantic Ridge). *Marine Ecology* **32**, 243–255. (doi:10.1111/j.1439-0485.2010.00431.x)

18. Embley R *et al.* 2007 Exploring the Submarine Ring of Fire: Mariana Arc - Western Pacific. *Oceanog.* **20**, 68–79. (doi:10.5670/oceanog.2007.07)

19. Kleint C *et al.* 2019 Geochemical characterization of highly diverse hydrothermal fluids from volcanic vent systems of the Kermadec intraoceanic arc. *Chemical Geology* **528**, 119289. (doi:10.1016/j.chemgeo.2019.119289)

20. Johnson SB, Won Y-J, Harvey JB, Vrijenhoek RC. 2013 A hybrid zone between Bathymodiolus mussel lineages from eastern Pacific hydrothermal vents. *BMC Evolutionary Biology* **13**, 21. (doi:10.1186/1471-2148-13-21)

21. Matabos M, Jollivet D. 2019 Revisiting the Lepetodrilus elevatus species complex (Vetigastropoda: Lepetodrilidae), using samples from the Galápagos and Guaymas hydrothermal vent systems. *Journal of Molluscan Studies* **85**, 66–72. (doi:10.1093/mollus/eyy061)

22. Breusing C, Johnson SB, Tunnicliffe V, Clague DA, Vrijenhoek RC, Beinart RA. 2020 Allopatric and sympatric drivers of speciation in alviniconcha hydrothermal vent snails. *Molecular Biology and Evolution* **37**, 3469–3484. (doi:10.1093/molbev/msaa177)

23. Castel J *et al.* 2022 Inter-Specific Genetic Exchange Despite Strong Divergence in Deep-Sea Hydrothermal Vent Gastropods of the Genus Alviniconcha. *Genes* **13**, 985. (doi:10.3390/genes13060985)

24. Thomas-Bulle C, Bertrand D, Nagarajan N, Copley RR, Corre E, Hourdez S, Bonnivard É, Claridge-Chang A, Jollivet D. 2022 Genomic patterns of divergence in the early and late steps of speciation of the deep-sea vent thermophilic worms of the genus Alvinella. *BMC Ecol Evo* **22**, 106. (doi:10.1186/s12862-022-02057-y)

25. Lunina AA, Vereshchaka AL. 2014 Distribution of hydrothermal alvinocaridid shrimps: Effect of geomorphology and specialization to extreme biotopes. *PLoS ONE* **9**. (doi:10.1371/journal.pone.0092802)

26. Methou P, Hernández-Ávila I, Cathalot C, Cambon-Bonavita M-A, Pradillon F. 2022 Population structure and environmental niches of Rimicaris shrimps from the Mid-Atlantic Ridge. *Marine Ecology Progress Series* **684**, 1–20. (doi:10.3354/meps13986)

27. Methou P, Chen C, Komai T. 2024 Revision of the alvinocaridid shrimp genus Rimicaris Williams & Rona, 1986 (Decapoda: Caridea) with description of a new species from the Mariana Arc hydrothermal vents. *Zootaxa* **5406**, 501–518. (doi:10.11646/zootaxa.5406.4.1)

28. Teixeira S, Serrão EA, Arnaud-Haond S. 2012 Panmixia in a fragmented and unstable environment: The hydrothermal shrimp Rimicaris exoculata disperses extensively along the Mid-Atlantic ridge. *PLoS ONE* **7**, 1–10. (doi:10.1371/journal.pone.0038521)

29. Beedessee G *et al.* 2013 High Connectivity of Animal Populations in Deep-Sea Hydrothermal Vent

Fields in the Central Indian Ridge Relevant to Its Geological Setting. *PLoS ONE* **8**, e81570. (doi:10.1371/journal.pone.0081570)

30. Zhou Y *et al.* 2022 Delineating biogeographic regions in Indian Ocean deep-sea vents and implications for conservation. *Diversity and Distributions* , 1–13. (doi:10.1111/ddi.13535)

31. Thaler AD, Plouviez S, Saleu W, Alei F, Jacobson A, Boyle EA, Schultz TF, Carlsson J, Van Dover CL. 2014 Comparative population structure of two deep-sea hydrothermal-vent- associated decapods (Chorocaris sp. 2 and Munidopsis lauensis) from southwestern Pacific back-arc basins. *PLoS ONE* **9**, 1–13. (doi:10.1371/journal.pone.0101345)

32. Yahagi T, Watanabe H, Ishibashi JI, Kojima S. 2015 Genetic population structure of four hydrothermal vent shrimp species (Alvinocarididae) in the Okinawa Trough, Northwest Pacific. *Marine Ecology Progress Series* **529**, 159–169. (doi:10.3354/meps11267)

33. Methou P, Ogawa NO, Nomaki H, Ohkouchi N, Chen C, Schnabel K. 2024 Genetic connectivity and isotopic niches of alvinocaridid shrimps from chemosynthetic habitats in Aotearoa/New Zealand, with a new Alvinocaris species. *Marine Ecology Progress Series* (doi:10.3354/meps14611)

34. Copley JTP, Young CM. 2006 Seasonality and zonation in the reproductive biology and population structure of the shrimp Alvinocaris stactophila (Caridea: Alvinocarididae) at a Louisiana Slope cold seep. *Marine Ecology Progress Series* **315**, 199–209. (doi:10.3354/meps315199)

35. Methou P, Chen C, Kayama H, Cambon M-A, Pradillon F. 2022 Reproduction in deep-sea vent shrimps is influenced by diet, with rhythms apparently unlinked to surface production. *Ecology and Evolution* , 1–12. (doi:10.1002/ece3.9076)

36. Methou P, Nye V, Copley JT, Watanabe HK, Nagai Y, Chen C. 2023 Life-history traits of alvinocaridid shrimps inhabiting chemosynthetic ecosystems around Japan. *Marine Biology* **170**, 1–17. (doi:10.1007/s00227-023-04221-4)

37. Stevens CJ, Limén H, Pond DW, Gélinas Y, Juniper SK. 2008 Ontogenetic shifts in the trophic ecology of two alvinocaridid shrimp species at hydrothermal vents on the Mariana Arc, western Pacific Ocean. *Marine Ecology Progress Series* **356**, 225–237. (doi:10.3354/meps07270)

38. Lupton J *et al.* 2006 Submarine venting of liquid carbon dioxide on a Mariana Arc volcano. *Geochem Geophys Geosyst* **7**, 2005GC001152. (doi:10.1029/2005GC001152)

39. Embley RW *et al.* 2006 Long-term eruptive activity at a submarine arc volcano. *Nature* **441**, 494–497. (doi:10.1038/nature04762)

40. Chadwick WW, Cashman KV, Embley RW, Matsumoto H, Dziak RP, De Ronde CEJ, Lau TK, Deardorff ND, Merle SG. 2008 Direct video and hydrophone observations of submarine explosive eruptions at NW Rota-1 volcano, Mariana arc. *J. Geophys. Res.* **113**, 2007JB005215. (doi:10.1029/2007JB005215)

41. Chadwick WW, Dziak RP, Haxel JH, Embley RW, Matsumoto H. 2012 Submarine landslide triggered by volcanic eruption recorded by in situ hydrophone. *Geology* **40**, 51–54. (doi:10.1130/G32495.1)

42. Schnur SR *et al.* 2017 A decade of volcanic construction and destruction at the summit of NW Rota-1 seamount: 2004–2014. *JGR Solid Earth* **122**, 1558–1584. (doi:10.1002/2016JB013742)

43. Williams AB, Dobbs FC. 1995 A new genus and species of caridean shrimp (Crustacea: Decapoda:

Bresiliidae) from hydrothermal vents on Loihi Seamount, Hawaii. *Proceedings of the Biological Society of Washington* **108**, 228–237.

44. Resing JA *et al.* 2011 Active submarine eruption of boninite in the northeastern Lau Basin. *Nature Geosci* **4**, 799–806. (doi:10.1038/ngeo1275)

45. Garcia MO, Caplan-Auerbach J, De Carlo EH, Kurz MD, Becker N. 2006 Geology, geochemistry and earthquake history of Lȍihi Seamount, Hawaìi's youngest volcano. *Geochemistry* **66**, 81–108. (doi:10.1016/j.chemer.2005.09.002)

46. Methou P, Michel LN, Segonzac M, Cambon-Bonavita M-A, Pradillon F. 2020 Integrative taxonomy revisits the ontogeny and trophic niches of Rimicaris vent shrimps. *Royal Society Open Science* **7**, 200837. (doi:10.1098/rsos.200837)

47. Puillandre N, Brouillet S, Achaz G. 2021 ASAP: assemble species by automatic partitioning. *Molecular Ecology Resources* **21**, 609–620. (doi:10.1111/1755-0998.13281)

48. Bandelt H-J, Forster P, Röhl A. 1999 Median-joining networks for inferring intraspecific phylogenies. *Molecular Biology and Evolution* **16**, 37–48. (doi:10.7882/FS.2004.039)

49. Leigh JW, Bryant D. 2015 POPART : full-feature software for haplotype network construction. *Methods in Ecology and Evolution* **6**, 1110–1116. (doi:10.1111/2041-210X.12410)

50. Rozas J, Ferrer-Mata A, Sanchez-DelBarrio JC, Guirao-Rico S, Librado P, Ramos-Onsins SE, Sanchez-Gracia A. 2017 DnaSP 6: DNA sequence polymorphism analysis of large data sets. *Molecular Biology and Evolution* **34**, 3299–3302. (doi:10.1093/molbev/msx248)

51. Tajima F. 1983 Evolutionary relationship of DNA sequences in finite populations. *Genetics* **105**, 437–460. (doi:10.1093/genetics/105.2.437)

52. Rambaut A. 2000 Estimating the rate of molecular evolution: incorporating non-contemporaneous sequences into maximum likelihood phylogenies. *Bioinformatics* **16**, 395–399. (doi:10.1093/bioinformatics/16.4.395)

53. Drummond AJ, Nicholls GK, Rodrigo AG, Solomon W. 2002 Estimating Mutation Parameters, Population History and Genealogy Simultaneously From Temporally Spaced Sequence Data. *Genetics* **161**, 1307–1320. (doi:10.1093/genetics/161.3.1307)

54. Pybus OG, Rambaut A. 2002 GENIE: estimating demographic history from molecular phylogenies. *Bioinformatics* **18**, 1404–1405. (doi:10.1093/bioinformatics/18.10.1404)

55. Shank TM, Black MB, Halanych KM, Lutz RA, Vrijenhoek RC. 1999 Miocene Radiation of Deep-Sea Hydrothermal Vent Shrimp (Caridea: Bresiliidae): Evidence from Mitochondrial Cytochrome Oxidase Subunit I. *Molecular Phylogenetics and Evolution* **13**, 244–254. (doi:10.1006/mpev.1999.0642)

56. Bianchini G, Sánchez-Baracaldo P. 2023 TreeViewer: Flexible, modular software to visualise and manipulate phylogenetic trees. *Ecology and Evolution* **14**, 1–16. (doi:10.1002/ece3.10873)

57. Meisner J, Albrechtsen A. 2018 Inferring Population Structure and Admixture Proportions in Low-Depth NGS Data. *Genetics* **210**, 719–731. (doi:10.1534/genetics.118.301336)

58. Gutenkunst RN, Hernandez RD, Williamson SH, Bustamante CD. 2009 Inferring the Joint

Demographic History of Multiple Populations from Multidimensional SNP Frequency Data. *PLoS Genet* **5**, e1000695. (doi:10.1371/journal.pgen.1000695)

59. Portik DM, Leaché AD, Rivera D, Barej MF, Burger M, Hirschfeld M, Rödel M, Blackburn DC, Fujita MK. 2017 Evaluating mechanisms of diversification in a Guineo-Congolian tropical forest frog using demographic model selection. *Molecular Ecology* **26**, 5245–5263. (doi:10.1111/mec.14266)

60. Skotte L, Korneliussen TS, Albrechtsen A. 2013 Estimating Individual Admixture Proportions from Next Generation Sequencing Data. *Genetics* **195**, 693–702. (doi:10.1534/genetics.113.154138)

61. Vieira FG, Lassalle F, Korneliussen TS, Fumagalli M. 2016 Improving the estimation of genetic distances from Next-Generation Sequencing data. *Biological Journal of the Linnean Society* **117**, 139–149. (doi:10.1111/bij.12511)

62. Charles KL *et al.* 2018 Sky, sea, and forest islands: Diversification in the African leaf-folding frog *Afrixalus paradorsalis* (Anura: Hyperoliidae) of the Lower Guineo-Congolian rain forest. *Journal of Biogeography* **45**, 1781–1794. (doi:10.1111/jbi.13365)

63. Wickham H *et al.* 2019 Welcome to the Tidyverse. *JOSS* **4**, 1686. (doi:10.21105/joss.01686)

64. R Core Team . 2021 R: A language and environment for statistical computing. See https://www.r-project.org.

65. Breusing C, Vrijenhoek RC, Reusch TBH. 2017 Widespread introgression in deep-sea hydrothermal vent mussels. *BMC Evolutionary Biology* **17**, 1–10. (doi:10.1186/s12862-016-0862-2)

66. Tran Lu Y A *et al.* 2024 Comparative population genomics unveils congruent secondary suture zone in Southwest Pacific Hydrothermal Vents. (doi:10.1101/2024.05.31.596862)

67. Barton NH, Hewitt GM. 1985 Analysis of Hybrid Zones. *Annual Review of Ecology and Systematics* **16**, 113–148.

68. Breusing C, Johnson SB, Tunnicliffe V, Vrijenhoek RC. 2015 Population structure and connectivity in Indo-Pacific deep-sea mussels of the Bathymodiolus septemdierum complex. *Conservation Genetics* **16**, 1415–1430. (doi:10.1007/s10592-015-0750-0)

69. Mitarai S, Watanabe H, Nakajima Y, Shchepetkin AF, McWilliams JC. 2016 Quantifying dispersal from hydrothermal vent fields in the western Pacific Ocean. *Proceedings of the National Academy of Sciences of the United States of America* **113**, 2976–2981. (doi:10.1073/pnas.1518395113)

70. Stankowski S, Westram AM, Zagrodzka ZB, Eyres I, Broquet T, Johannesson K, Butlin RK. 2020 The evolution of strong reproductive isolation between sympatric intertidal snails. *Phil. Trans. R. Soc. B* **375**, 20190545. (doi:10.1098/rstb.2019.0545)

71. Ribardière A, Daguin-Thiébaut C, Houbin C, Coudret J, Broudin C, Timsit O, Broquet T. 2017 Geographically distinct patterns of reproductive isolation and hybridization in two sympatric species of the *Jaera albifrons* complex (marine isopods). *Ecology and Evolution* **7**, 5352–5365. (doi:10.1002/ece3.3106)

72. Székely T, Weissing FJ, Komdeur J. 2014 Adult sex ratio variation: Implications for breeding system evolution. *Journal of Evolutionary Biology* **27**, 1500–1512. (doi:10.1111/jeb.12415)

73. Grant PR, Grant BR. 2019 Adult sex ratio influences mate choice in Darwin's finches. *Proceedings*

of the National Academy of Sciences of the United States of America **116**, 12373–12382. (doi:10.1073/pnas.1903838116)

74. Correa C, Thiel M. 2003 Mating systems in caridean shrimp (Decapoda: Caridea) and their evolutionary consequences for sexual dimorphism and reproductive biology. *Revista Chilena de Historia Natural* **76**, 187–203. (doi:10.4067/S0716-078X2003000200006)

75. Brunner O, Chen C, Giguère T, Kawagucci S, Tunnicliffe V, Kayama H, Satoshi W. 2022 Species assemblage networks identify regional connectivity pathways among hydrothermal vents in the Northwest Pacific. *Ecology and Evolution* , 1–15. (doi:10.1002/ece3.9612)

76. Stern RJ, Fouch MJ, Klemperer SL. 2003 An overview of the Izu-Bonin-Mariana subduction factory. In *Geophysical Monograph Series* (ed J Eiler), pp. 175–222. Washington, D. C.: American Geophysical Union. (doi:10.1029/138GM10)

77. Hall R. 2002 Cenozoic geological and plate tectonic evolution of SE Asia and the SW Paci®c: computer-based reconstructions, model and animations. *Journal of Asian Earth Sciences*

78. Crawford WC, Hildebrand JA, Dorman LM, Webb SC, Wiens DA. 2003 Tonga Ridge and Lau Basin crustal structure from seismic refraction data. *J. Geophys. Res.* **108**, 2001JB001435. (doi:10.1029/2001JB001435)

79. Sun S, Sha Z, Wang Y. 2018 Phylogenetic position of Alvinocarididae (Crustacea: Decapoda: Caridea): New insights into the origin and evolutionary history of the hydrothermal vent alvinocarid shrimps. *Deep-Sea Research Part I: Oceanographic Research Papers* **141**, 93–105. (doi:10.1016/j.dsr.2018.10.001)

80. Schweitzer CE, Feldmann RM, Audo D, Charbonnier S, Garassino A, Schweigert G, Sudarsky S. 2023 Treatise Online no. 175: Part R, Revised, Volume 1, Systematic descriptions: Infraorders Procaridea, Stenopodea, Caridea. *TREON* (doi:10.17161/to.vi.21568)

81. Hernández-Ávila I, Cambon-Bonavita MA, Pradillon F. 2015 Morphology of first zoeal stage of four genera of alvinocaridid shrimps from hydrothermal vents and cold seeps: Implications for ecology, larval biology and phylogeny. *PLoS ONE* **10**, 1–27. (doi:10.1371/journal.pone.0144657)